COMPUTER VISION AND IMAGE UNDERSTANDING
Vol. 64, No. 3, November, pp. 305–322, 1996
ARTICLE NO. 0062

Geometric Heat Equation and Nonlinear Diffusion of Shapes and Images

BENJAMIN B. KIMIA* AND KALEEM SIDDIQI†

*Division of Engineering, Brown University, Providence, Rhode Island 02912; and †Department of Electrical Engineering, McGill University, Montreál, Québec, H3A 2A7, Canada

Received January 18, 1994; accepted February 8, 1995

Visual tasks often require a hierarchical representation of shapes and images in scales ranging from coarse to fine. A variety of linear and nonlinear smoothing techniques, such as Gaussian smoothing, anisotropic diffusion, regularization, etc., have been proposed, leading to scalespace representations. We propose a *geometric* smoothing method based on local curvature for shapes and images. The deformation by curvature, or the geometric heat equation, is a special case of the *reaction–diffusion* framework proposed in [41]. For shapes, the approach is analogous to the classical heat equation smoothing, but with a renormalization by arc-length at each infinitesimal step. For images, the smoothing is similar to anisotropic diffusion in that, since the component of diffusion in the direction of the brightness gradient is nil, edge location is left intact. Curvature deformation smoothing for shape has a number of desirable properties: it preserves inclusion order, annihilates extrema and inflection points without creating new ones, decreases total curvature, satisfies the semigroup property allowing for local iterative computations, etc. Curvature deformation smoothing of an image is based on viewing it as a collection of iso-intensity level sets, each of which is smoothed by curvature. The reassembly of these smoothed level sets into a smoothed image follows a number of mathematical properties; it is shown that the extension from smoothing shapes to smoothing images is mathematically sound due to a number of recent results [21]. A generalization of these results [14] justifies the extension of the entire *entropy scale space* for shapes [42] to one for images, where each iso-intensity level curve is deformed by a combination of constant and curvature deformation. The scheme has been implemented and is illustrated for several medical, aerial, and range images.

1. INTRODUCTION

Shapes and images are often perceived as a hierarchical structure of elements. It has been argued that recognition of objects should rely on a representation that captures this structure in a hierarchy of ''scale.'' The basic idea is to introduce a family of shapes, or images, which progressively become simpler in the sense that ''significant'' features remain while the less significant ones vanish [71, 58, 49, 90]. Witkin proposed that the convolution of a signal with a Gaussian removes small-scale features, namely, zero-crossings, while retaining the more significant ones [88]. Koenderink showed that among the linear operators the heat (diffusion) equation and its associated Gaussian kernel is the only sensible way of smoothing images, by demanding that the process satisfy the properties of *causality*, *homogeneity*, and *isotropy* [48, 50]. These properties require that ''structure'' is not created with increasing scale and that operations are homogeneous in space and direction; see also [9]. Yuille and Poggio presented scaling theorems for zero-crossings [89], and Hummel and Monoit showed that zero-crossings, when supplemented with gradient data along the zero-crossing boundaries, are sufficient to reconstruct the original signal. Recently Florack *et al.* have provided a physical motivation and mathematical basis for a scale-space representation [25], arriving at the Gaussian family of filters *without* an explicit requirement for causality. In the discrete domain, Lindeberg has formulated a scale-space by discretizing the underlying diffusion equation [52, 53]. The kernel of the discretized equation is related to modified Bessel functions of integer order. For a recent review of linear scale-space theory see [54, 55].

In addition to image intensity, scale-spaces have also been constructed for shapes. Asada and Brady [8] smooth the curvature function to obtain a hierarchy of features. Mokhtarian and Mackworth [60] smooth the coordinates by a Gaussian filter. Horn and Weldon [34] point to the shrinkage problems of this method and propose instead to filter the extended circular image of the curve with a Gaussian filter. This method avoids the shrinkage problem, but appears to be applicable only to convex curves. Lowe, on the other hand, corrects for the shrinkage problem by inflating the curve proportional to the curvature of the smoothed curve, which indicates how much shrinkage has occurred. Oliensis [64] suggests that this is the case only for small curvature and proposes instead to maintain the low frequencies exactly, while preserving the local nature of the process. The resulting filter is similar to Meyer's wavelet transform [59]. In the context of a theory of mea-

1077-3142/96 $18.00

surement, Koenderink and van Doorn embed a shape in a morphogenetic sequence based on the Gaussian [50].

Recently, a number of nonlinear diffusion techniques have been proposed to deal with the shortcomings of the linear smoothing techniques. These are summarized in Section 6. Our proposal for smoothing shapes and images is also nonlinear and is related to the idea of diffusion and the associated Gaussian kernel. To smooth shapes, we deform the boundary along the normal proportional to its curvature. This leads to the geometric heat equation which, as we will mathematically show, has many desirable smoothing properties. On the other hand, to smooth images, each iso-intensity level set is considered as a shape, a view afforded by properties of the smoothing process, as we shall show, and whose smoothing leads to remarkable results. The curvature deformation smoothing method is related to the linear heat equation smoothing and to anisotropic diffusion. The method has been implemented and applied to several shapes and range and intensity images. In fact, the extension of curvature deformation of shapes to curvature deformation of images can be generalized to a combination of constant and curvature deformation, leading to an *entropy scale space* [42] for images.

The paper is organized as follows. In Section 2 the *shape from deformation framework* as originally presented in [39, 41, 38] and later developed in [7, 42–47] is briefly reviewed. The focus of this paper is a special case of the reaction–diffusion space, namely, when the shape is deformed only by curvature deformation, giving rise to the geometric heat equation. In Section 3 a number of desirable properties of this nonlinear smoothing process are presented. In Section 4 the idea of smoothing of shapes by curvature deformation is extended to the smoothing of images. In Section 5 the connection between the geometric heat equation (curvature deformation) smoothing and the classical heat equation (Gaussian smoothing) is shown for shapes. Section 6 shows the connection to anisotropic diffusion. Finally, in Section 7 the process is illustrated on a number of shapes and images, and comparisons are made with some other techniques.

2. THE SHAPE FROM DEFORMATION FRAMEWORK

In this section we review a framework for representing two-dimensional shape designed to capture its essence in relation to ''nearby'' shapes. The geometric curvature deformation is a special case of this framework and provides a smoothing process for shape. We will then extend the idea to smoothing intensity and range images by considering their iso-intensity level sets as shapes.

Robust recognition under variations in the visual scene, such as changes in viewpoint and viewing direction, object movement, and growth, demands that shapes be represented not *statically* as a set of unrelated primitives, but *dynamically* in a rich sequence of shapes [50]. In a dynamic representation each shape is related to its ''closest'' neighbors giving rise to a topology for shape. Unfortunately, standard geometries do not support such a topology for recognition [47]. Alternatively, shape can be studied in the context of *deformations* of it. Observing that slight changes in the shape boundary often causes slight changes in the shape itself, we proceed to deform the shape boundary in an arbitrarily general fashion,

$$\begin{cases} \dfrac{\partial \mathscr{C}}{\partial t} = \alpha(s,t)\vec{T} + \beta(s,t)\vec{N} \\ \mathscr{C}(s,0) = \mathscr{C}_0(s), \end{cases} \tag{1}$$

where $\mathscr{C}$ is the boundary vector of coordinates, $\vec{T}$ is the tangent, $\vec{N}$ is the outward normal, s is the path parameter, t is the time duration (magnitude) of the deformation, and α, β are arbitrary functions. This, by a reassignment (i.e., reparametrization) of points, can be reduced to [39, 38, 28, 20]

$$\begin{cases} \dfrac{\partial \mathscr{C}}{\partial t} = \beta(s,t)\vec{N} \\ \mathscr{C}(s,0) = \mathscr{C}_0(s), \end{cases} \tag{2}$$

where β is again arbitrary, but not necessarily the same as that of the previous equation. This form of deformation embeds certain known techniques in image processing. For example, taking the deformation to be constant, $\beta = \pm 1$, gives the prairie fire model of Blum [11]. As another example, deformations which are functions of the local orientation of the curve tangent, θ,

$$\begin{cases} \dfrac{\partial \mathscr{C}}{\partial t} = \beta(\theta(s,t))\vec{N} \\ \mathscr{C}(s,0) = \mathscr{C}_0(s), \end{cases} \tag{3}$$

embed *all* algebraic set-theoretic convex morphological operations, but now in a geometric, differential setting [7]. On the other hand, deformations that depend on the derivative of orientation, curvature κ, smooth shapes and images in interesting ways which are similar to Gaussian smoothing, but have better properties, as we shall see in this paper. The intrinsic[1] deformation by curvature, or that which depends only on the *local geometry* of the curve [19], was proposed in [39, 41] as

[1] Deformations that do not depend on the coordinate system.

$$\begin{cases} \dfrac{\partial \mathscr{C}}{\partial t} = \beta(\kappa(s,t))\vec{N} \\ \mathscr{C}(s,0) = \mathscr{C}_0(s). \end{cases} \tag{4}$$

A special case of this deformation is when the deformation is a linear function of curvature $\beta(\kappa) = \beta_o - \beta_1\kappa$; see [39, 42, 44–47]:

$$\begin{cases} \dfrac{\partial \mathscr{C}}{\partial t} = (\beta_0 - \beta_1\kappa)\vec{N} \\ \mathscr{C}(s,0) = \mathscr{C}_0(s). \end{cases} \tag{5}$$

The space of all possible deformations in this form is spanned by two parameters, the ratio of the coefficients β_0/β_1 and time, t, constituting the two axes of the *reaction–diffusion space*. Underlying the representation of shape in this space are a set of *shocks* [51], or entropy-satisfying singularities, which develop during the evolution. The set of shocks which form along the reaction axis, $\beta_1 = 0$, is indeed the *skeleton* proposed by Blum [11]. Shocks also form along other axes of the reaction–diffusion space and are the key to representing shape. To continue the evolution beyond these singularities, the classical notions of normal, curvature, etc. are considered in the *generalized* or *weak* sense by using the concepts of entropy and viscosity solutions [56, 16, 36, 14]. For theoretical as well as numerical reasons the original curve flow is embedded in the level set evolution of an evolving surface [67, 78–80]. Let the surface be denoted by $z = \phi(x, y, t)$ with the correspondence that the evolving shape is represented at all times by its zero level set $\phi(x, y, t) = 0$. It can be shown that the zero level set of surfaces evolving according to

$$\phi_t + \beta(\kappa)\,|\nabla\phi| = 0 \tag{6}$$

correspond to the viscosity solutions of (4) [10].

To relate this shock-based representation of shape to smoothing, the *entropy scale-space* [42, 46] has been derived from the reaction–diffusion space. In the entropy scale space shapes are smoothed using a combination of reaction ($\beta_1 = 0$), and diffusion ($\beta_0 = 0$): reaction operates through the formation of shocks which act as black holes, locally annihilating information; diffusion operates through the global spreading and subsequent blending of information along the boundary.

The focus of this paper is a study of curvature deformation, i.e., when $\beta_0 = 0$. Since the magnitude of β_1 is redundant as it is captured by the time parameter t, and $\beta_1 < 0$ corresponds to an unstable inverse operator, let $\beta_1 = 1$:

$$\begin{cases} \dfrac{\partial \mathscr{C}}{\partial t} = -\kappa\vec{N} \\ \mathscr{C}(s,0) = \mathscr{C}_0(s). \end{cases} \tag{7}$$

The curvature deformation equation (7), known as the curve shortening flow, has been extended to an affine invariant flow, $\partial\mathscr{C}/\partial t = -\kappa^{1/3}\vec{N}$, by Sapiro and Tannenbaum [72, 73, 75] and independently by Alvarez *et al.* [3]. The surface evolution corresponding to (7) is derived from (6) as

$$\phi_t - \kappa\,|\nabla\phi| = 0. \tag{8}$$

Since

$$\kappa = \frac{(\phi_{xx}\phi_y^2 - 2\phi_{xy}\phi_x\phi_y + \phi_{yy}\phi_x^2)}{(\phi_x^2 + \phi_y^2)^{3/2}}, \tag{9}$$

we have

$$\phi_t = \frac{(\phi_{xx}\phi_y^2 - 2\phi_{xy}\phi_x\phi_y + \phi_{yy}\phi_x^2)}{(\phi_x^2 + \phi_y^2)}. \tag{10}$$

We now consider curvature deformation in the context of smoothing shapes and images. For shapes, we will construct the surface ϕ from the distance transform of the shape [47]. For intentisty or range images it is mathematically valid to directly obtain the surface ϕ from the grey-level information, as we shall see in Section 4. Each level set is then "smoothed" by curvature deformation. We now discuss properties of this process in addition to its connection to several standard smoothing techniques.

3. NONLINEAR SMOOTHING BY CURVATURE DEFORMATION

In this section, we discuss a number of interesting properties of smoothing by curvature deformation of the contours of a shape. First, shapes preserve their inclusion order when smoothed, without self-intersecting. Second, all shapes smooth to round points (points that dilate to circles) without developing singularities or self-intersections. Third, the total curvature is strictly decreasing in the smoothing process, unless the curve is a circle in which case it is a constant. Fourth, the number of curvature extrema and inflection points is strictly decreasing, unless the curve is a circle. Fifth, this process satisfies the semigroup property and as such can be implemented as a local iteration, and is well suited to parallel implementation. Finally, the process can easily be modified in the context of the reaction–diffusion space to include area-preserving smoothing.

1. *Order-Preserving Smoothing*

The curvature deformation evolution (7), which is a special axis of the reaction–diffusion space [47], is known as the "curve-shortening flow" in differential geometry. In the process of curvature deformation disjoint closed curves

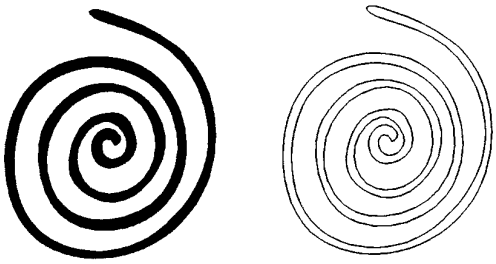

FIG. 1. Will the boundary of the above shape evolve to a circular point without developing self-intersections? Grayson showed that the high curvature end points will move in much faster than the low curvature points in such a way that self-intersections are avoided. Eventually, the shape evolves to a round point, keeping the boundaries apart in the process!

remain disjoint; this follows from an application of the maximum principle for parabolic differential equations [70, 86]. As a result, two shapes, one inside another, will never cross in the process of smoothing; see Section 4 for a more detailed analysis.

2. *Smooth Smoothing*

A shape lasts only a finite time under curvature deformation smoothing. This is a consequence of the inclusion order-preserving property; since any closed curve can be considered inside some large circle with a finite evolution time, and since a circle lasts only for a finite time, the original curve can also only last for a finite time under curvature deformation. This finite evolution time under curvature deformation naturally raises three interesting questions: First, must every curve collapse to a point, or can it collapse to a set of points, or segments? Second, if a curve must collapse to a point, will the limit point be round?[2] Third, will the curve develop self-intersections or become singular in the process?

There has been a growing interest in these questions in differential geometry for the past decade. Gage and Hamilton [26, 27, 29] answered these questions for a convex curve and showed that it must evolve to a round point without developing self-intersections or singularities. Grayson [31] generalized this result to show that *any* embedded curve will become convex without developing self-intersections or singularities; after this Gage and Hamilton's results apply. To appreciate the significance of this theorem examine the spiral shape in Fig. 1, which must evolve to a circular point. We now state the theorem as derived in Grayson [31].

THEOREM 1. *Let* $\mathscr{C}(s, 0)$: $S^1 \to \mathbf{R}^2$ *be a parametrized smooth embedded curve in the plane. Then there exists some* $T > 0$, *and* $\mathscr{C}$: $S^1 \times [0, T) \to \mathbf{R}^2$, *such that*

$$\frac{\partial \mathscr{C}}{\partial t} = -\kappa \vec{N}, \tag{11}$$

$\mathscr{C}(s, t)$ *is smooth for all* t, *it converges to a point as* $t \to T$, *and its limiting shape as* $t \to T$ *is a round circle, with convergence in the* $\mathscr{C}^\infty$ *norm.*

3. *Decreasing Total Curvature*

A measure of complexity for a shape is the total curvature of its boundary. Total curvature $\overline{\kappa}$ is defined as

$$\overline{\kappa} = \int_0^{2\pi} |\kappa|\, g\, ds = \int_0^L |\kappa|\, d\tilde{s}, \tag{12}$$

where g is the metric (speed) $|\partial \mathscr{C}/\partial s|$, $\tilde{s}$ is the arc-length parameter, and L is the length of the boundary. A curve which has a larger number of undulations has a larger total curvature; for convex curves, $\overline{\kappa} = 2\pi$. The following theorem [80, 44] shows that all noncircular embedded curves evolving by curvature-dependent deformation (5), with $\beta_1 > 0$, have strictly decreasing total curvature. A circle is the only curve for which total curvature remains constant, $\overline{\kappa} = 2\pi$.

THEOREM 2. *Let a family of curves satisfy* (7) *for which* $\beta_1 > 0$. *Then, if* $\kappa_{\tilde{s}}(\tilde{s}, t) \neq 0$ *for all* $\tilde{s}$ *and all* $t > 0$

$$\overline{\kappa}(t) < \overline{\kappa}(0). \tag{13}$$

4. *Annihilation of Extrema and Inflection Points*

Another issue of concern is whether new curvature extrema or inflection points can be created in the process of smoothing. Theorem 3 shows that no new curvature extrema or inflection points can be created [46]. Since the total curvature is strictly decreasing for noncircular shapes, we conclude that existing extrema and zeros of curvature must also disappear in time.

THEOREM 3. *Let a family of curves satisfy* (7) *for which* $\beta_1 > 0$. *Then, the number of curvature extrema* (*vertices*) *is a nonincreasing function of time. Similarly, the number of zeros of curvature is a nonincreasing function of time.*

COROLLARY 1. *The number of maxima, minima, and zeros of curvature for a noncircular curve is strictly decreasing; circles lack such points and will evolve none.*

5. *Iterative Smoothing*

Ideally a smoothing process should be implementable locally and iteratively. A property that would make this possible is the *semigroup* property: Operators T with a size

[2] A limit point is round if when dilated it becomes a circle. To visualize a nonround point, say a triangular point, consider a triangle evolving by scaling down and eventually shrinking to a point. The limit point is not round, but triangular.

or scale parameter t which satisfy $T(t_1 + t_2) = T(t_2)T(t_1)$ are said to form a *semigroup*. For example, Gaussian smoothing, or linear convolution of a function with the Gaussian, satisfies the semigroup property since $[f(s) * K(s, t_1)] * K(s, t_2) = f(s) * K(s, t_1 + t_2)$. This implies that to smooth by amount $2t$ one can smooth by t in two sequential steps. There is great computational savings in doing so since the effective width of a Gaussian is much smaller for smaller steps. Similarly, deformation by curvature also satisfies the semigroup property [21]:

THEOREM 4. *Let $T(t)$ be the operator that evolves an initial curve $\mathscr{C}_0$ to $\mathscr{C}_t$ by curvature, i.e., $\mathscr{C}_t = T(t)\mathscr{C}_0$. Then $T(t + s) = T(t)T(s)$.*

As such, the process can be implemented *locally* and *iteratively*, with the potential of parallelization.

6. *Other Properties*

In addition to the properties already discussed, it is interesting to note that curvature deformation is the *fastest* way to shrink the length of a curve [28]. The speed of shrinkage of length, among all curves of length L, is slowest for the circle. However, the enclosed area decreases at a constant rate which equals the total curvature of the curve. This shrinkage effect occurs in other smoothing operators and various solutions have been proposed; see, for example, [57] for a way to deal with Gaussian smoothing shrinkage effects, and [18] for the use of intrinsic polynomial stabilizers. Alternatively, one can use results suggested by Gage to overcome this effect: he defined an ''area-preserving'' flow by subtracting the component of the length gradient which lies parallel to the area gradient [28]: $L_t = -\int \langle \mathscr{C}_t, \kappa\vec{N}\rangle\, ds$, $A_t = -\int \langle \mathscr{C}_t, \vec{N}\rangle\, ds$, where L is the length and A is the area of the curve. This leads to the evolution

$$\mathscr{C}_t = \left(\kappa - \frac{2\pi}{L}\right)\vec{N}, \tag{14}$$

namely, the gradient flow of the length functional among curves of a fixed area. Alternatively, Gage [28] proposed to magnify the plane by a homothety simultaneously with the evolution, leading to

$$\mathscr{C}_t = \left(\kappa - \frac{\pi p}{A}\right)\vec{N} + \alpha\vec{T}, \tag{15}$$

where p is the support function of $\mathscr{C}$ given by $-\langle \mathscr{C}, \vec{N}\rangle$; the tangential component does not change the shape as explained earlier. The results due to Gage are applied to the smoothing of shapes [74]. In our framework, flows that preserve area, length, and other similar functionals are special cases in the reaction–diffusion space, where β_0 is now a function of length. Note, however, that the length and area measures are *global* and are therefore seriously affected by changes in the scene, e.g., partial occlusion, movement of parts, etc. The fact that such global measures can become variable under visual transformations motivates the use of the *full* reaction–diffusion space. In this context, the evolution of a partially occluded shape by some ratio β_0/β_1 will match the evolution of the full shape with a different one.

4. SMOOTHING IMAGES VIA LEVEL SET DEFORMATION

The smoothing of a shape by curvature deformation of its boundary can be extended to the smoothing of images. Recall that curve deformation is implemented as the evolution of a surface which embeds the evolving curve as its zero level set. Until now the initial surface was obtained from the distance transform of the shape, for convenience. However, as we shall shortly show, since any continuous surface can be used, this additional degree of freedom enables gray-level intensity or range information to be represented. Our view of smoothing images, then, is to smooth each iso-intensity level set by curvature-dependent deformation, in analogy to binary shapes. The smoothed image is then obtained by superimposing the smoothed level sets, Fig. 2. Before we may proceed with this approach to smoothing images, however, a number of essential properties must be established. Here we should mention the recent elegant approach of Alvarez *et al.* in formalizing the properties of scale space for images [1, 2–6].

The first and second theorems allow us to consider images where each iso-intensity level set may have singularities, e.g., corners, disconnected pieces, etc., by viewing the surface evolution in a ''weak'' sense [56, 17, 33, 15, 51, 36]. The third theorem shows that the smoothing of each iso-intensity contour is independent of the image itself, Fig. 6. The fourth theorem shows that the evolution process is order preserving and does not allow iso-intensity level sets to cross. In fact, although iso-intensity level sets may initially share segments in common due to discretization, the fifth theorem shows that these will pull apart after smoothing. The last theorem ensures that iso-intensity level sets never move closer to one another than they were initially. These recent mathematical results provide a theoretical justification for extending shape smoothing via curvature deformation to image smoothing via the curvature deformation of its iso-intensity level sets.

Consider the parabolic partial differential equation

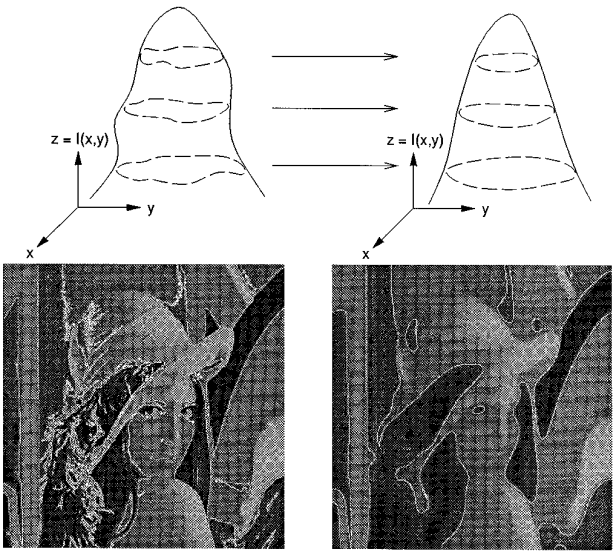

FIG. 2. This figure illustrates the extension from shapes to images of smoothing by curvature deformation. An intensity image is represented as a surface and each level set is smoothed by curvature deformation. The smoothed image is obtained by superimposing the smoothed level sets. For illustration, we superimpose level set 75 in white on an image (bottom left), and a curvature deformation smoothed version of it (bottom right).

$$\begin{aligned} \phi_t &= |\nabla\phi| \operatorname{div}\left(\frac{\nabla\phi}{|\nabla\phi|}\right) \quad \text{in } \mathbf{R}^n \times [0, \infty), \\ \phi &= \phi_0 \qquad\qquad\qquad\quad \text{on } \mathbf{R}^n \times \{t = 0\} \end{aligned} \tag{16}$$

for the hypersurface $\phi = \phi(x, t)$, $(x \in \mathbf{R}^n, t \geq 0)$, where ϕ_0: $\mathbf{R}^n \to \mathbf{R}$ is some continuous function such that ϕ_0 is constant on $\mathbf{R}^n \cap \{|x| \geq S\}$, for some $S > 0$. This equation evolves each level set of ϕ according to its mean curvature, at least where ϕ is smooth and its gradient does not vanish. In our case, $n = 2$, (16) reduces to (10). We now restate a number of useful and relevant properties for $n = 2$,

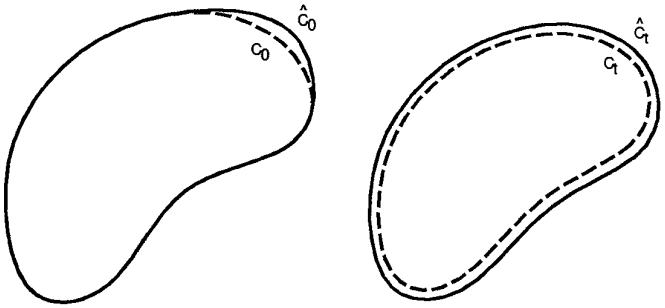

FIG. 3. Initially overlapping contours separate during curvature deformation, i.e., if $\mathscr{C}_0 \subseteq \hat{\mathscr{C}}_0$ but $\mathscr{C}_0 \neq \hat{\mathscr{C}}_0$, the two curves will pull apart instantly, even when $\mathscr{C}_0$ and $\hat{\mathscr{C}}_0$ coincide except for a small region [21].

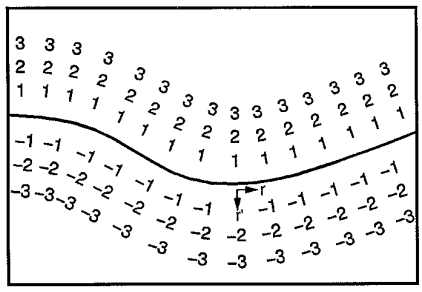

FIG. 4. This figure depicts the signed distance function ϕ in the neighborhood of a shape's boundary; r' is the direction of $\nabla\phi$ and r is perpendicular to r'.

which were established in [21] for general n. $\mathscr{C}_0$ denotes a particular level set of ϕ_0 and $\mathscr{C}_t$ is its evolution in time.

THEOREM 5. *A "weak" solution to* (16) *exists and is unique.*

It is important to consider the evolution in the weak sense, in the context of "viscosity solutions" of nonlinear partial differential equations [56, 15–17, 37, 36]. This allows us to consider shapes that have corners or discontinuities in orientation where, for example, the classical notion of a normal is not well defined. However, we are assured that when the classical solution exists, it coincides with the weak solution:

THEOREM 6. *The evolution by curvature* (16) *agrees with the classical motion by curvature, if and so long as the latter exists.*

We are assured by Theorem 7 that the choice of a different surface ϕ_0', which embeds the same contour as a level set, will lead to the same smoothing of that contour.

THEOREM 7. *The evolution of $\mathscr{C}_0$ into $\mathscr{C}_t$ is independent of the choice of the initial function ϕ_0.*

This important result, namely, that the evolution of a level set by its curvature is *independent* of the choice of ϕ_0, underlies our approach to smoothing images. Observe that if we select the image intensity function as the surface ϕ_0, each iso-intensity level set of ϕ_0 will evolve by curvature, exhibiting all the desirable properties detailed in Section 3. This is equivalent to evolving each iso-intensity curve *separately* by curvature, see Fig. 6, but with significant computational savings. This approach exhibits properties of anisotropic diffusion for images, see Section 6.

THEOREM 8. *If $\mathscr{C}_0$ and $\hat{\mathscr{C}}_0$ are two compact subsets of $\mathbf{R}^2$ such that $\mathscr{C}_0 \subseteq \hat{\mathscr{C}}_0$ then the subsequent evolutions $\mathscr{C}_t$ and $\hat{\mathscr{C}}_t$ of $\mathscr{C}_0$ and $\hat{\mathscr{C}}_0$ satisfy $\mathscr{C}_t \subseteq \hat{\mathscr{C}}_t$.*

It is clear that in the continuous domain, the iso-intensity contours of an image are isolated and nonoverlapping.

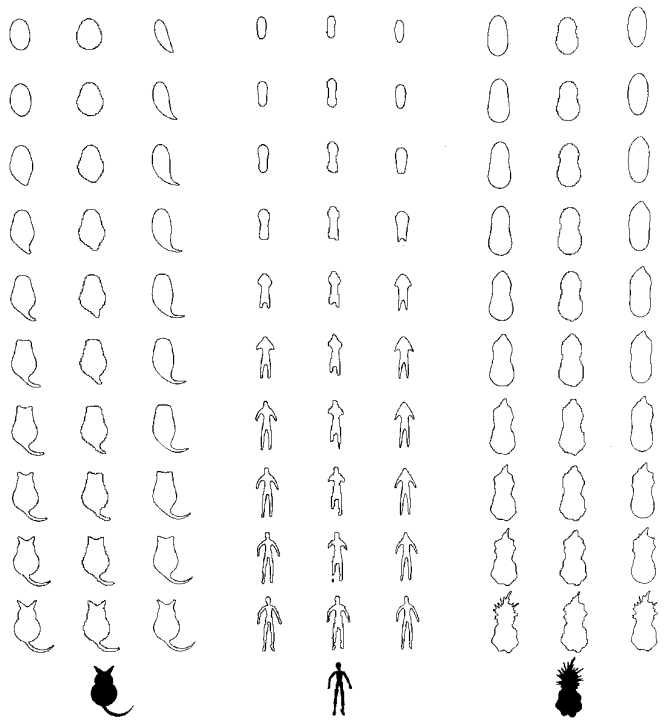

FIG. 5. This figure illustrates curvature deformation (left columns), region blurring (middle columns), and boundary blurring (right columns) for the cat, doll, and pear images, respectively.

Conversely, for a collection of level sets to represent iso-intensity contours of an image, they too must be nonoverlapping. Theorem 8 assures us that the level sets maintain this property during evolution by curvature deformation. We had earlier referred to this property as inclusion order preserving, Section 3. Whereas iso-intensity contours are separated in the continuous domain, in the discrete domain some level sets may partially overlap. Theorem 9 assures us that so long as such level sets do not cross, they will separate in the course of the evolution, Fig. 3.

THEOREM 9. *Given two initial curves $\mathscr{C}_0$ and $\hat{\mathscr{C}}_0$ such that $\mathscr{C}_0 \subseteq \hat{\mathscr{C}}_0$ but $\mathscr{C}_0 \neq \hat{\mathscr{C}}_0$, their evolutions $\mathscr{C}_t$ and $\hat{\mathscr{C}}_t$ do not coincide for any $t > 0$.*

In fact, Theorem 10 guarantees that two level sets cannot move closer to one another than they were initially.

THEOREM 10. *Assume $\mathscr{C}_0$ and $\hat{\mathscr{C}}_0$ are nonempty compact sets in $\mathbf{R}^2$ and $\{\mathscr{C}_t\}_{t>0}$ and $\{\hat{\mathscr{C}}_t\}_{t>0}$ are the subsequent generalized motions by curvature. Then dist$(\mathscr{C}_0, \hat{\mathscr{C}}_0) \leq$ dist$(\mathscr{C}_t, \hat{\mathscr{C}}_t)$ for $t \geq 0$.*

Whereas thus far we have specialized to the case of curvature deformation, a number of the above properties hold for a larger, more general class of geometric parabolic partial differential equations [14, 13, 30]. This includes the evolution of each level set of ϕ by a combination of constant and curvature deformation (5), where ϕ evolves according to (6), with $\beta(\kappa) = \beta_0 - \beta_1\kappa$. In particular, a unique weak solution exists, and the evolution of each level set of ϕ is independent of that of the other level sets. As a consequence, the extension of curvature deformation of shapes to curvature deformation of images may be generalized to a combination of constant and curvature deformation, leading to an *entropy scale-space* [42] for images. Examples are shown in Section 7.

5. CONNECTION TO THE HEAT EQUATION AND GAUSSIAN SMOOTHING

The connection between the deformation of a curve by its curvature (7), namely, the geometric heat equation, and the classical heat equation can be easily shown. Assume arc-length parametrization, $\tilde{s}$, so that

$$\left|\frac{\partial \mathscr{C}}{\partial \tilde{s}}\right| = 1. \tag{17}$$

Then,

$$\begin{aligned} \vec{T} &= \frac{\partial \mathscr{C}}{\partial \tilde{s}} \\ \kappa &= \left|\frac{\partial \vec{T}}{\partial \tilde{s}}\right| \\ \vec{N} &= -\frac{\partial \vec{T}}{\partial \tilde{s}} \Big/ \left|\frac{\partial \vec{T}}{\partial \tilde{s}}\right|. \end{aligned} \tag{18}$$

Since $\kappa\vec{N} = -\partial\vec{T}/\partial\tilde{s} = -\partial^2\mathscr{C}/\partial\tilde{s}^2$, $\partial\mathscr{C}/\partial t = -\kappa\vec{N}$ leads to

$$\begin{aligned} \frac{\partial \mathscr{C}}{\partial t} &= \frac{\partial^2 \mathscr{C}}{\partial \tilde{s}^2}, \\ \frac{\partial \mathscr{C}}{\partial t} &= \Delta \mathscr{C}, \end{aligned} \tag{19}$$

which is the diffusion (heat) equation for the coordinates. Note that this equation holds only for an infinitesimal time step, since arc-length is not preserved. The enforcement of arc-length parametrization requires a coupling of (19) with $|\mathscr{C}_{\tilde{s}}| = 1$. In this sense the system is not linear.

To show the connection with the classical heat equation, let us first examine Gaussian-based smoothing of a shape's coordinates. Mokhtarian and Macworth use the Gaussian to create a scale-space for shapes [60] by convolving it with the original coordinate functions $\mathscr{C}_0(s) = (x_0(s), y_0(s))$. They track inflection points of smoothed coordinate functions over time.

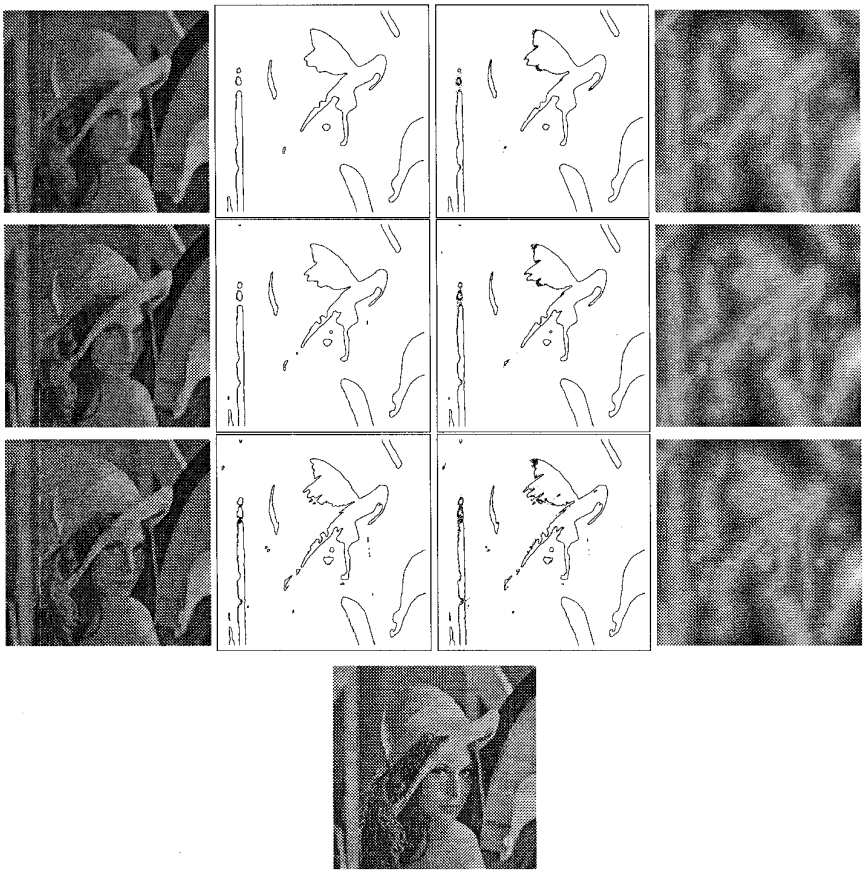

FIG. 6. This figure illustrates that each iso-intensity level set is smoothed independently of the rest of the image. Bottom: The original image. First column (bottom to top): The sequence of curvature deformation smoothed images. Second column (bottom to top): A particular level set of the smoothed images in column one (intensity = 125). Recall that this level set is the evolution by curvature deformation of the original image's level set (intensity = 125). Third column (bottom to top): The evolution by curvature of the same level set, but now with a different surface (obtained from the distance transform). Fourth column (bottom to top): The evolved distance transform surface corresponding to the images in column three. Whereas the evolved surfaces in the first and fourth columns differ, the corrspondence between the second and third columns numerically confirms the theoretical independence of level set evolution from the original image, Theorem 7.

$$\begin{aligned} x(s,t) &= x_0(s) * K(s,t) \\ y(s,t) &= y_0(s) * K(s,t), \end{aligned} \tag{20}$$

where t is the extent of the Gaussian $K(s, t)$. It is well known [87] that the Gaussian

$$K(s,t) = \frac{1}{(4\pi t)^{1/2}} e^{-s^2/4t} \tag{21}$$

is the heat kernel. In other words (20) is equivalent to

$$\frac{\partial \mathscr{C}}{\partial t} = \frac{\partial^2 \mathscr{C}}{\partial s^2}. \tag{22}$$

Equations (19) and (22) appear similar. Indeed, in the short time, since arc-length is approximately preserved, the two smoothing processes are similar. However, for longer smoothing time, the two processes diverge in effect. For example, evolutions by (22) can cause self-intersections. In addition, they place too much significance on elongated features; the remedy is to renormalize for arc-length in each step [61], effectively yielding Eq. (19).

A second connection between curvature deformation and Gaussian smoothing is based on "volumetric blurring" [48, 50], where the focus is on the blurring of the region rather than the boundary. For example, let ϕ_0 be the characteristic function of the original shape, i.e., ϕ_0 has value 1 inside the shape and value 0 otherwise. The shape may then be smoothed by iteratively blurring the characteristic function as follows:

$$\phi_{n\Delta t}(x, y) = \begin{cases} 1 & \text{where } \phi_{(n-1)\Delta t}(x,y) * K(x,y,\Delta t) \geq 0.5 \\ 0 & \text{otherwise.} \end{cases} \tag{23}$$

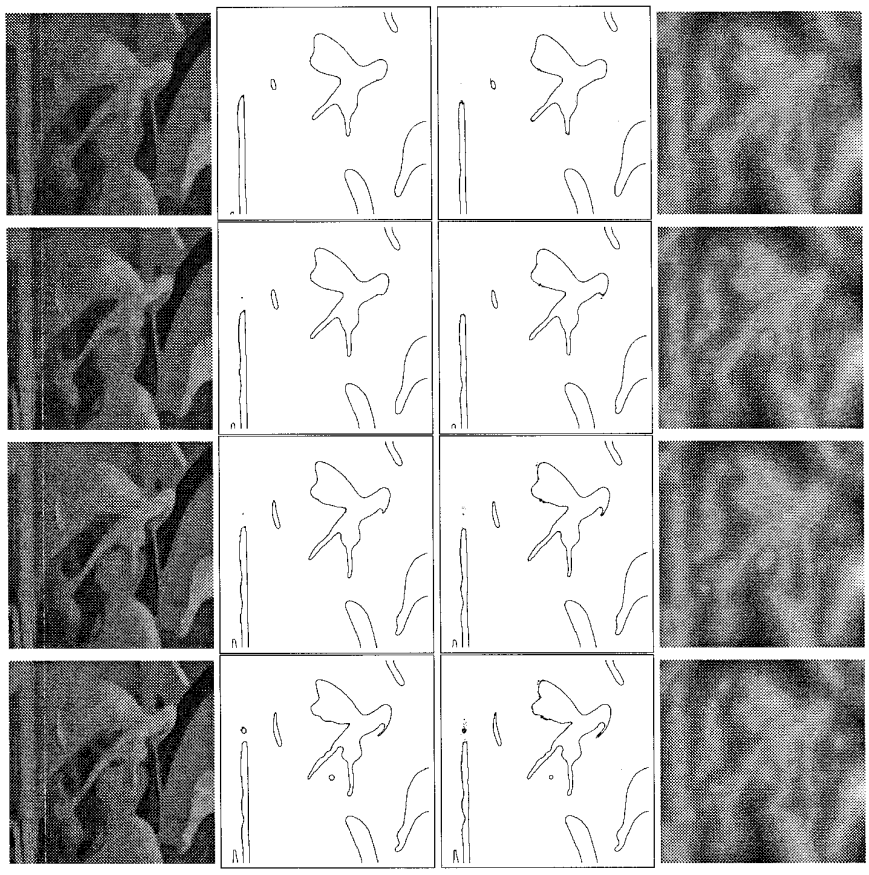

FIG. 6—*Continued*

Here $K(x, y, \Delta t)$ denotes a 2D Gaussian centered at (x, y) with extent Δt, and the smoothed shape is the boundary of the blurred characteristic function. Note that at each time step, a new characteristic function is computed by thresholding the blurred characteristic function from the previous time step. Figure 5 depicts the outcome of this process for three different shapes.

The relationship between the above form of region blurring and the evolution of the shape's boundary by curvature is as follows. In [22] Evans and Spruck show that under mean curvature evolution, for small times the signed distance function d of $\mathscr{C}_t$ satisfies a nonlinear parabolic equation of the form $\partial d/\partial t = F(D^2 d, d)$. They then show that for small times and for a small neighborhood around the initial curve $\mathscr{C}_0$, the initial signed distance function evolving according to $\partial d/\partial t = F(D^2 d, d)$, subject to unit gradient boundary conditions, remains the signed distance function to a curve evolving by mean curvature. Moreover,

$$\frac{\partial d}{\partial t} = \Delta d \tag{24}$$

on the evolving curve. Hence, Evans and Spruck's results imply that in the limit as the time step becomes very small, region blur as described by (23), but with ϕ equal to the signed distance function d, is equivalent to curvature deformation.

An intuitive explanation of this result is as follows [3]. The heat equation may be written as $\phi_t = \Delta\phi = \phi_{rr} + \phi_{r'r'}$, where r and r' are any two orthogonal directions. Let r' be the direction of $\nabla\phi$. If we specialize to the case of the signed distance function as ϕ, Fig. 4, we see that near the shape's boundary, $|\phi_{r'}| = 1$. Consequently, $\phi_{r'r'}$ is zero near the boundary. Now recall that curvature deformation satisfies (10), which we restate:

$$\begin{aligned} \phi_t &= \kappa\,|\nabla\phi|, \\ &= \frac{(\phi_{xx}\phi_y^2 - 2\phi_{xy}\phi_x\phi_y + \phi_{yy}\phi_x^2)}{(\phi_x^2 + \phi_y^2)^{3/2}}\,|\nabla\phi|. \end{aligned} \tag{25}$$

Here ϕ is any continuous surface, including but not limited to the signed distance function, whose level sets evolve by mean curvature. Let θ be the angle that r forms with the x-axis. The second directional derivative in the direction r can be written as

$$\phi_{rr} = \phi_{xx}\cos^2(\theta) + 2\phi_{xy}\cos(\theta)\sin(\theta) + \phi_{yy}\sin^2(\theta). \tag{26}$$

With r perpendicular to the direction of $\nabla\phi$, we have $(\cos(\theta), \sin(\theta)) = (-\phi_y/(\phi_x^2 + \phi_y^2)^{1/2}, \phi_x/(\phi_x^2 + \phi_y^2)^{1/2})$ and infer

$$\kappa = \frac{\phi_{rr}}{(\phi_x^2 + \phi_y^2)^{1/2}} = \frac{\phi_{rr}}{|\nabla\phi|}, \tag{27}$$

or substituting in (25)

$$\phi_t = \phi_{rr}. \tag{28}$$

Therefore, the approaches of curvature deformation and iterated region blur converge when ϕ is the signed distance function.

6. CONNECTION TO ANISOTROPIC DIFFUSION

A number of linear scale spaces have been introduced to combat noise as well as to hierarchically structured features. Perona and Malik [68] noted a problem with the standard scale spaces for edges, namely, a shift in the true location of edges in scale. This is primarily due to the homogeneity of the Gaussian operator with respect to edges, which implies that Gaussian blur does not respect image boundaries. The Gaussian operator was originally proposed as the unique linear operator that satisfies the *causality*, *homogeneity*, and *isotropy* criteria [48]. Perona and Malik replace the latter two, which were originally proposed to simplify the problem, with two new ones, *immediate localization* and *piecewise smoothing*. To achieve these objectives, consider the anisotropic diffusion equation

$$\phi_t = \mathrm{div}(c(x, y, t)\,\nabla\phi) = c(x, y, t)\,\Delta\phi + \nabla c \cdot \nabla\phi, \tag{29}$$

where ϕ denotes brightness intensity. Observe that if image boundaries are known, then setting the diffusion coefficient c to zero at the boundaries and one at the interior of each region will smooth within each region independently of other regions, without smearing edges. Note, however, that the solution involves the original problem of detecting boundaries! Instead, Perona and Malik rely on a best estimate of where these boundaries may be by relating c to some nonnegative monotonically decreasing function of edge strength, where edge strength is measured by the gradient of the image:

$$c(x, y, t) = g(|\nabla\phi(x, y, t)|). \tag{30}$$

As a consequence, regions of low brightness gradients are blurred, while regions of high gradient values are not. The edges of the resulting image are enhanced in time and regions converge to regions of constant intensity.

Catté *et al.* [12] point out two limitations of the Perona–Malik scheme. First, "noise introduces very large, in theory unbounded, oscillations of the gradient," leading to the enhancement of noise edges, which will then be kept. These edges are in practice filtered by a first stage smoothing, which in turn introduces an additional parameter. The second problem is theoretical in that for the suggested choices of g no correct theory is available for the existence and uniqueness of the solutions. This leads to the possibility that pictures close in norm can lead to drastically different edge maps. They propose a slight modification where the gradient $|\nabla\phi(x, y, t)|$ in (30) is replaced with a Gaussian smoothed estimate $|DG_\sigma * \phi(x, y, t)|$, leading to

$$\phi_t = \mathrm{div}(g(|DG_\sigma * \phi(x, y, t)|)\,\nabla\phi). \tag{31}$$

In other words, the initial smoothing of Perona and Malik is now integrated into the scheme. Catté *et al.* then prove the existence, uniqueness, and regularity properties of solutions of (31). Hence, the above two problems are avoided. A similar idea is proposed by Whitaker and Pizer [85], where the extent of the Gaussian is itself a decreasing function of time. See also [84].

The connection between regularization and anisotropic diffusion is addressed by Nordström [63] and Shah [81]. Nordström shows that the (stochastic or variational) regularization approach [83] of global minimization of the sum of an edge term, a deviation from original image term, and a smoothness or likelihood term, has a differential counterpart obtained by the Euler–Lagrange equation. This local condition is very much like the Perona–Malik anisotropic diffusion with an additional *bias* term which moderates the diffusion when the diffused function drifts far away from the original image. However, Catté *et al.* [12] raise the same stability issue and in addition argue that the maximum principle used in this work is generally not valid.

Shah suggests the minimization of two coupled energy functionals whose first variations lead to

$$\begin{aligned} \frac{\partial\phi'}{\partial t} &= v^2\,\Delta\phi' - \frac{1}{\sigma^2}(\phi' - \phi) \\ \frac{\partial v}{\partial t} &= \rho\,\Delta v - \frac{v}{\rho} + 2\alpha(1 - v)|\nabla\phi'|. \end{aligned} \tag{32}$$

Here ϕ is the original image intensity function, ϕ' is a smoothed version of ϕ, and v is a "discontinuity indicator" whose value is close to 1 in the vicinity of a discontinuity and is close to 0 otherwise. The first of these equations leads to a smoothing of the image, where the $1/\sigma^2(\phi' -$

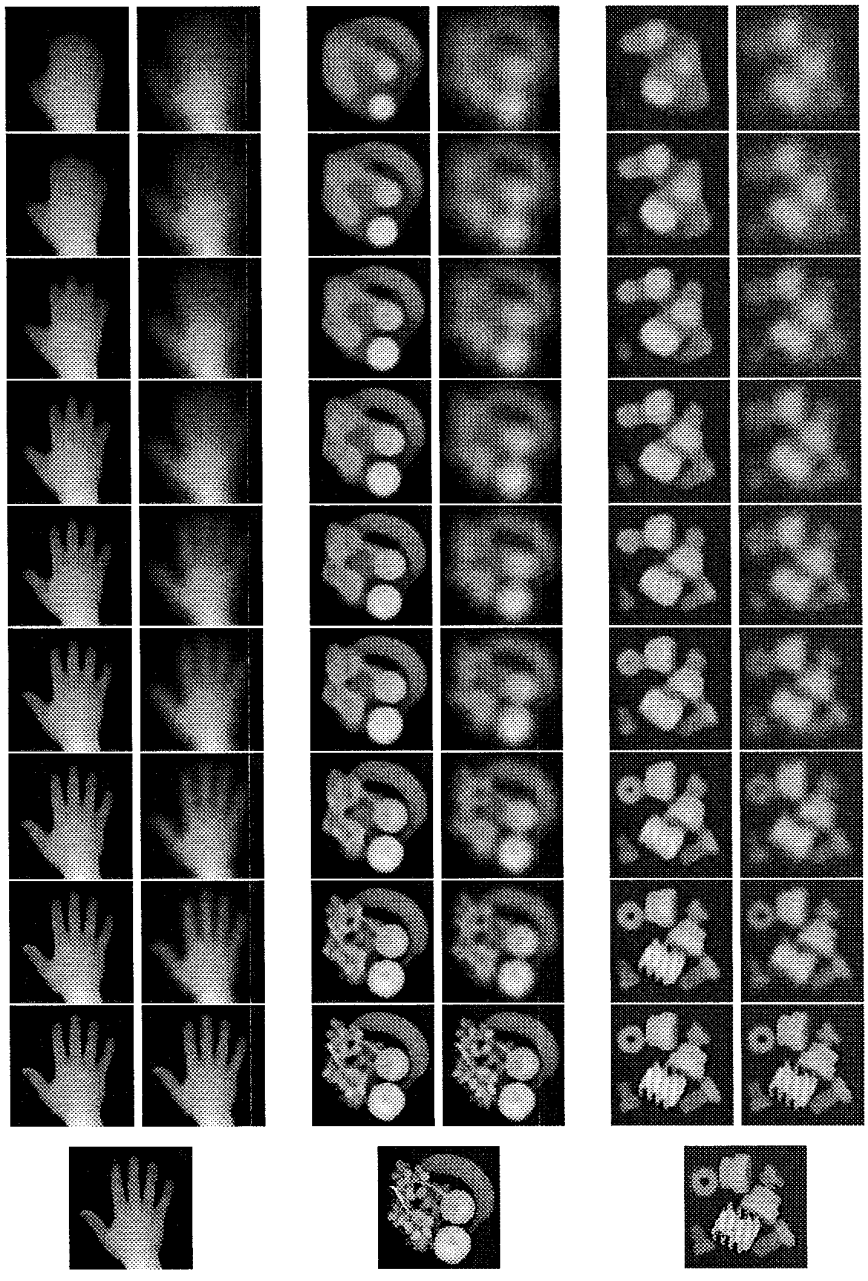

FIG. 7. Curvature deformation verses Gaussian blurring of an image. Bottom: Original images. Left columns: Curvature deformation. Right columns: Gaussian blurring. Observe how in contrast to Gaussian blurring, edges remain crisp for curvature deformation.

ϕ) term is similar to Nordström's bias term. The second equation leads to a smoothing of the boundaries.

Proesmans *et al.* [69] observe that since diffusion equations smooth, Shah's approach can not lead to edge enhancement. Moreover, the smoothing of v leads to a loss of boundary localization. They suggest a modification where the $\Delta\phi'$ term in (32) is replaced by Perona and Malik's $\mathrm{div}(c(\phi')\ \nabla\phi')$, leading to a process that encourages edge sharpening in regions nearby discontinuities. Several variants of these coupled nonlinear diffusion equations are presented. For improved response in the neighborhood of ramp edges as well as contrast enhancement, second-order smoothing processes are proposed; these minimize a functional of the second derivative of the image intensity.

Alternatively, Osher and Rudin view enhancement and segmentation as a kind of "deblurring," which they implement using a conservative numerical scheme [66]. This

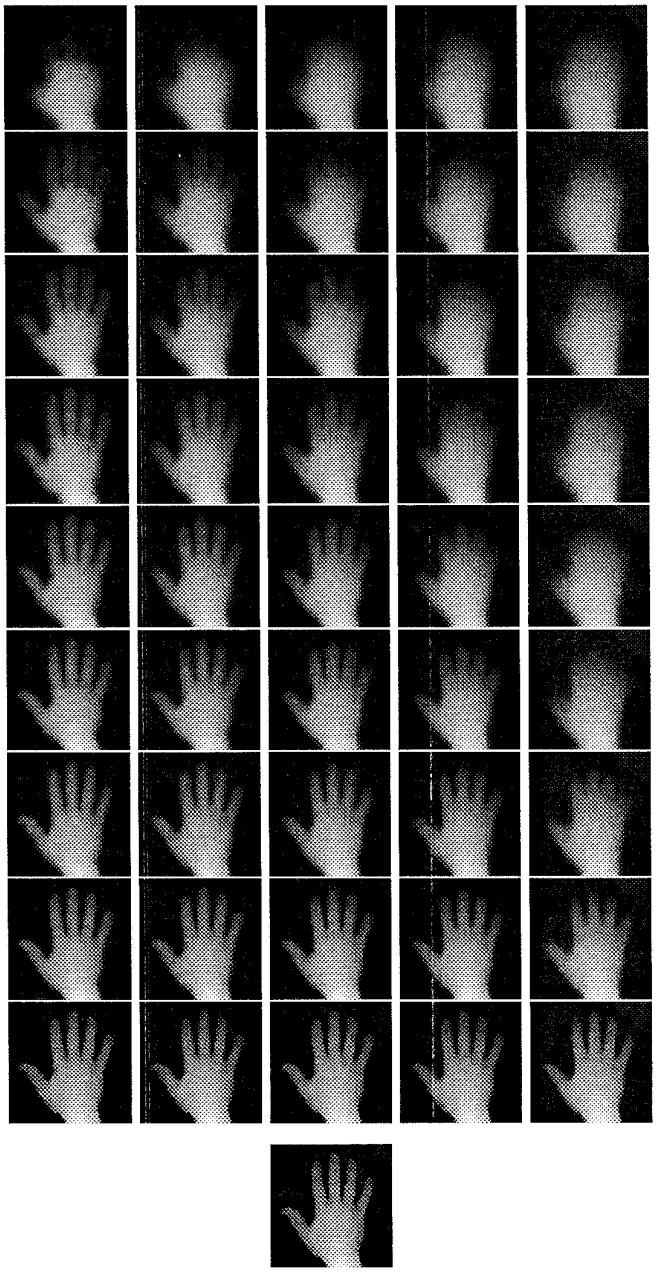

FIG. 8. An extension of curvature deformation to a combination of constant and curvature deformation leads to an entropy scale space [42] for images. Bottom: Original image. Left column (bottom to top): Constant deformation only. Left to right (bottom to top): Increasing amounts of curvature deformation.

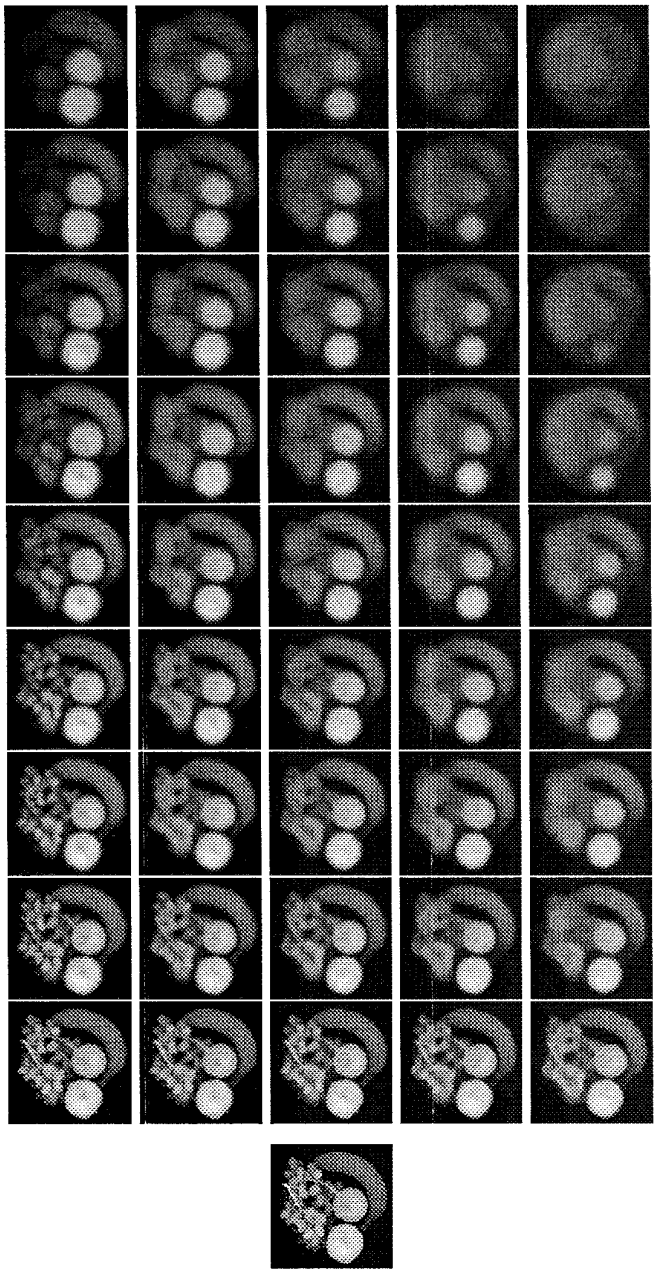

FIG. 9. An extension of curvature deformation to a combination of constant and curvature deformation leads to an entropy scale space [42] for images. Bottom: Original image. Left column (bottom to top) Constant deformation only. Left to right (bottom to top): Increasing amounts of curvature deformation.

conservative scheme resembles the inverse heat equation as closely as possible; see also [35].

Alvarez *et al.* [5] study a class of nonlinear parabolic differential equations specified by

$$\phi_t = g(|G * \nabla\phi|)|\nabla\phi| \operatorname{div} \frac{\nabla\phi}{|\nabla\phi|}, \quad \phi(x, y, 0) = \phi_0(x, y), \qquad (33)$$

where G is a smoothing kernel, say the Gaussian, and $g(\xi)$ is a nonincreasing real function which tends to zero as $\xi \to 0$. They then show the existence and uniqueness of the viscosity solution of this equation. Our curvature deformation is related to (33) in that $g(\cdot) = 1$ ($g(\xi)$ does not tend to zero as $\xi \to 0$). However, the theory of viscosity solutions of the curvature deformation, known as the

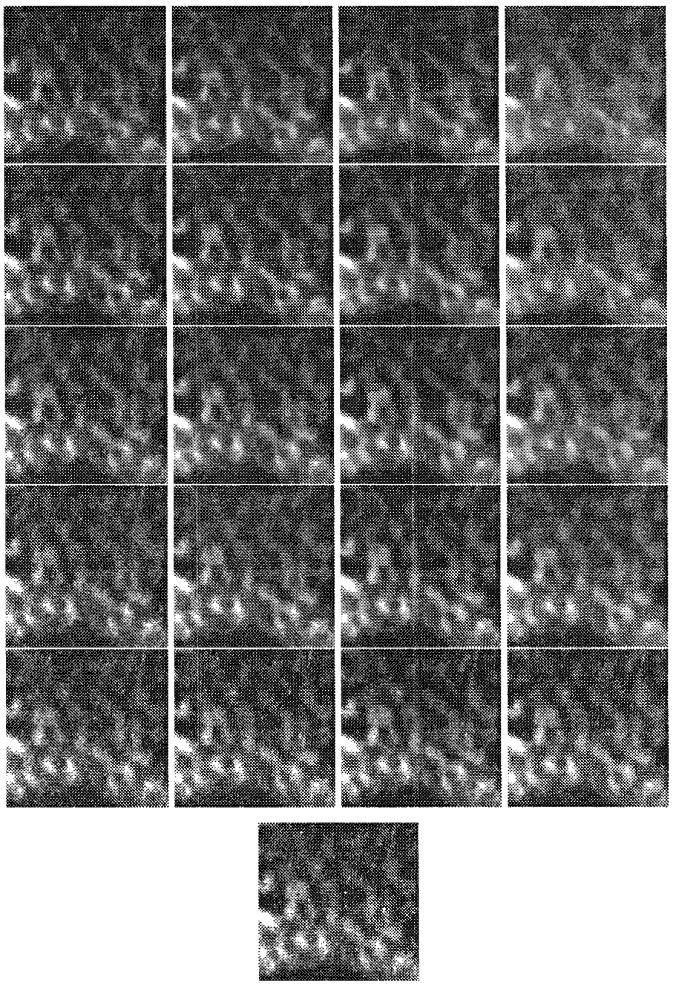

FIG. 10. An extension of curvature deformation to a combination of constant and curvature deformation leads to an entropy scale space [42] for images. Bottom: The original image is a portion of the medical image in Fig. 12. Left column (bottom to top): Constant deformation only. Left to right (bottom to top): Increasing amounts of curvature deformation.

"mean curvature flow," was addressed previously [21–23, 14, 13], and was numerically demonstrated by Osher and Sethian [67].

To see how curvature deformation preserves edges while smoothing, recall that under this process, $\phi_t = \phi_{rr}$ (28), where r is the direction perpendicular to the image intensity gradient $\nabla\phi$. In contrast to the heat equation, $\phi_t = \Delta\phi = \phi_{rr} + \phi_{r'r'}$, where r and r' are any two orthogonal directions, we observe that curvature deformation ignores the diffusion term $\phi_{r'r'}$ in the direction r' of the brightness gradient, and as such does not allow diffusion across edges [5]. Edge location and sharpness are left intact since, in effect, the component of diffusion along the gradient has been subtracted off. This is similar to Perona and Malik's approach in that the edges are preserved. However, "noise edges" are not amplified because curvature deformation does not enhance edges. This is the anisotropic diffusion connection.

Finally, we should mention that recently Florack *et al.* have proposed a unifying framework for a variety of nonlinear diffusion models [24]. Here the idea of a "generalized" scale-space is introduced, where each nonlinear scale-space formally corresponds to a transformation of a linear one.

7. EXAMPLES

In this section we discuss implementation issues and illustrate the scheme with several examples. Since curvature deformation smoothes singularities and no new singularities can form, a central difference scheme is sufficient to robustly simulate the process. See [62] for a framework

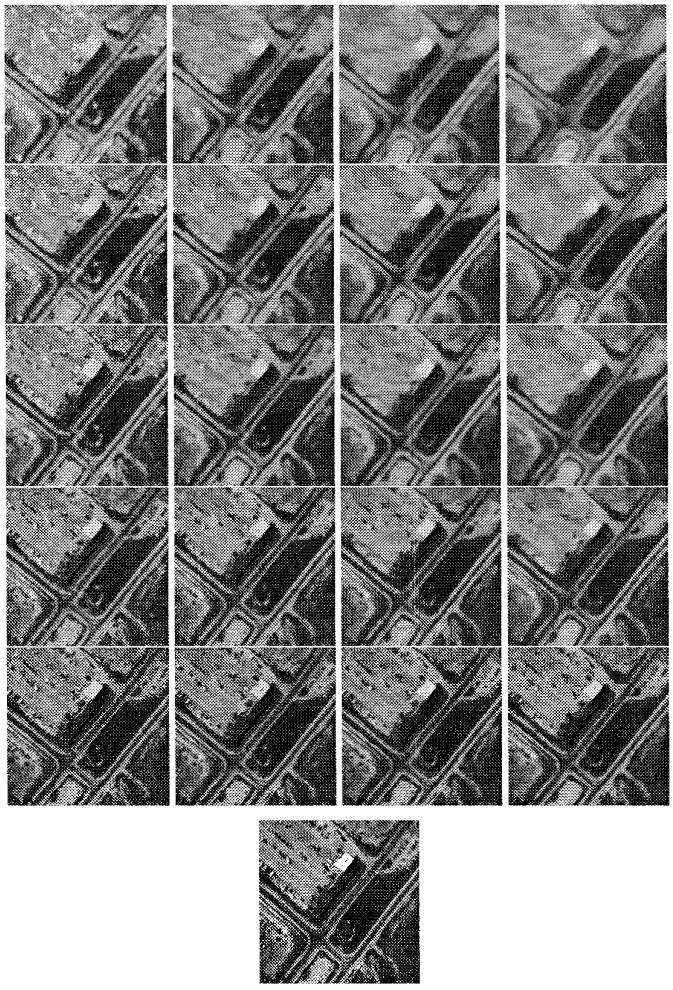

FIG. 11. An extension of curvature deformation to a combination of constant and curvature deformation leads to an entropy scale space [42] for images. Bottom: The original image is a portion of the aerial image in Fig. 13. Left column (bottom to top): Constant deformation only. Left to right (bottom to top): Increasing amounts of curvature deformation.

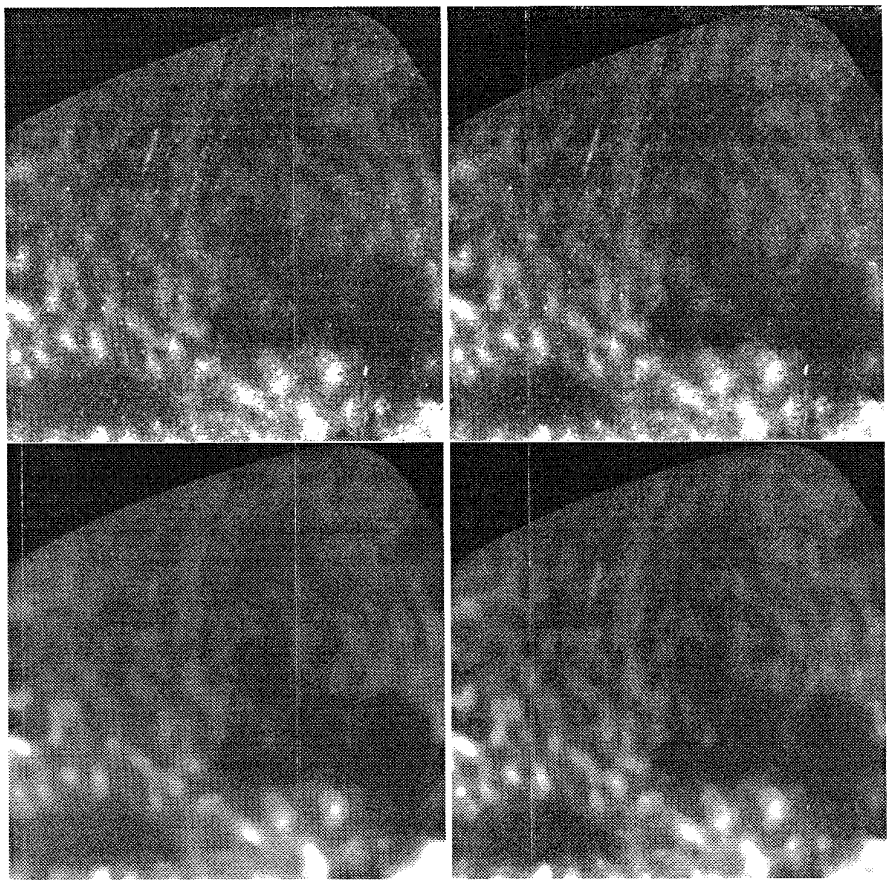

FIG. 12. This figure illustrates geometric smoothing for a medical image. Top left: Original MRI image of a brain slice. Clockwise from top right: Curvature deformation eliminates noise and enhances the ocular dominance columns. It is instructive to visually track an edge as the image is smoothed; slowly curving edges remain sharp while edges corresponding to smaller structures are removed.

for implementing this and other nonlinear diffusion schemes, based on the notion of well-posed differentiation by Gaussian kernels. Note that in contrast to curvature deformation, evolutions involving constant deformation (hyperbolic) may lead to the formation of singularities. As such, shock-capturing numerical schemes are required for the full reaction–diffusion space spanning constant and curvature deformation. High-resolution schemes were proposed by Harten, and Osher and Chakravarthy [32, 65] and applied to front propagation by Osher and Sethian [67, 76–80]. These schemes have been used for shape representation in computer vision [39, 41] and can be applied to a variety of other computer vision applications [82].

The numerical scheme for curvature deformation *requires no parameters.* The magnitude of β_1 is absorbed in the time parameter t and only affects the speed of smoothing. The original shape/image is evolved over time, producing a sequence of fine to coarse smoothed shapes/images. We illustrate this smoothing process on a variety of shapes and images.

Figure 5 compares the curvature deformation of a shape with Gaussian blurring of its region and its boundary, respectively. Observe that boundary blurring can place too much emphasis on elongated features, e.g., the tail of the cat, while region blurring can lead to topological splits, e.g., the hands and feet of the doll. On the other hand, curvature deformation exhibits the desirable properties discussed in Section 3, in particular, each shape becomes round in the limit.

Figure 6 demonstrates that each iso-intensity level set evolves independently of the original image. To illustrate this point, a level set of the original image (intensity = 125) was smoothed using the original image as the surface as well as by constructing an artificial surface from it (obtained from the distance transform). The numerical simulation confirms the theoretical results, Theorem 7.

Figure 7 compares curvature deformation smoothing with Gaussian blurring for three range images. Gaussian blurring smoothes equally well within regions and across edges, e.g., the fingers of the hand are blurred together. In contrast, curvature deformation exhibits properties of anisotropic diffusion, smoothing within but not between

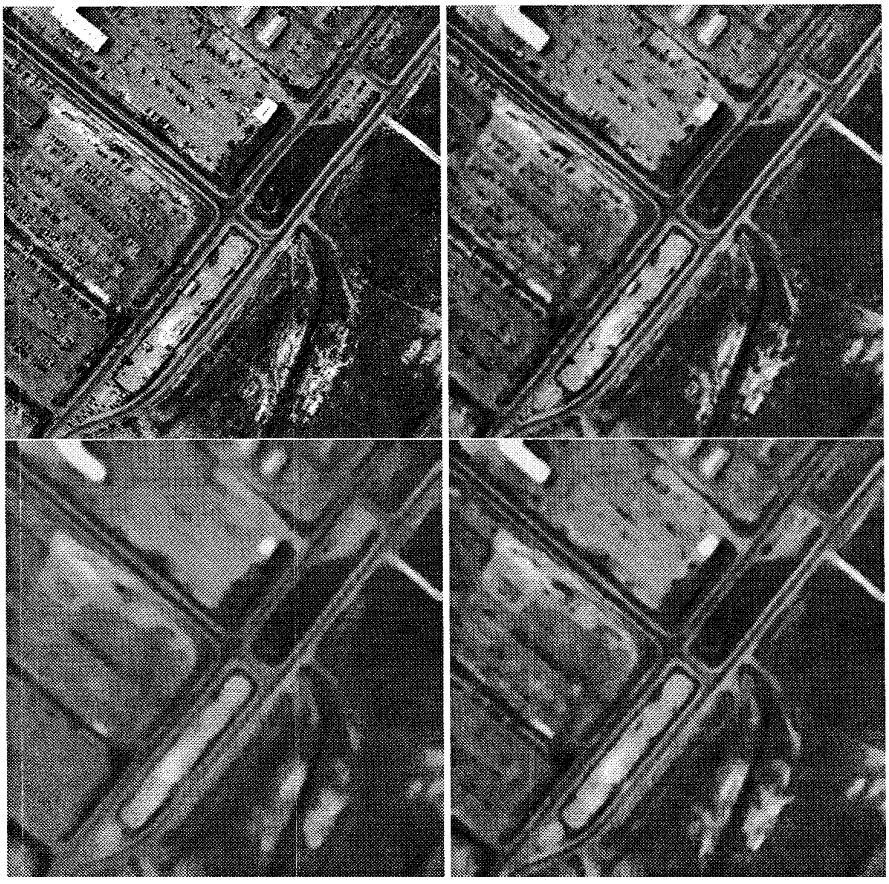

FIG. 13. This figure illustrates geometric smoothing of an aerial image. Top left: Original aerial image taken from the ARPA RADIUS program. Clockwise from top right: Curvature deformation smoothing of the original. Note how small structures within large blocks are removed while slowly curving edges remain sharp.

regions; observe that the fingers of the hand remain separate.

Figures 8–11 illustrate the extension from shapes to images of a combination of constant and curvature deformation, leading to an entropy scale space [42] for images. Under curvature deformation, all iso-intensity curves are smoothed to circles which eventually disappear. In contrast, constant deformation in the entropy scale space leads to the ''breaking off'' of structures: small structures such as the fingers of the hand (Fig. 8, left column), or the grapes (Fig. 9, left column) disappear while the larger structures are left intact.

Figure 12 depicts an application of curvature deformation smoothing to the medical domain. The task here is to measure the width of the ocular dominance columns. The ocular dominance bands, however, are congested with small structures such as blood vessels. Observe how curvature deformation smoothes over these small structures while preserving the more slowly curving edges of the ocular dominance columns, making the bands distinct in the process. Experts working with these images consider the results desirable.

Figure 13 depicts an application of curvature deformation smoothing to an aerial image taken from the ARPA RADIUS program. Again, small structures such as cars are smoothed over while the edges of more slowly curving structures such as blocks and roads are preserved and remain sharp. Note that the emphasis is on the ''geometry'' of the object rather than on pure edge contrast.

Figure 14 compares curvature deformation with Perona and Malik's anisotropic diffusion [68] for a portion of the aerial image in Fig. 13. Anisotropic diffusion can be made to preserve all sharp edges, including those of small structures such as the cars, by selecting a conductance function g that drops sharply with increasing image intensity gradient (left column). Alternatively, such small structures can be smoothed over by selecting a less steep conductance function, but at the expense of also smoothing over the edges of larger structures such as the roads (middle column). Curvature deformation, which is based on the geometry of

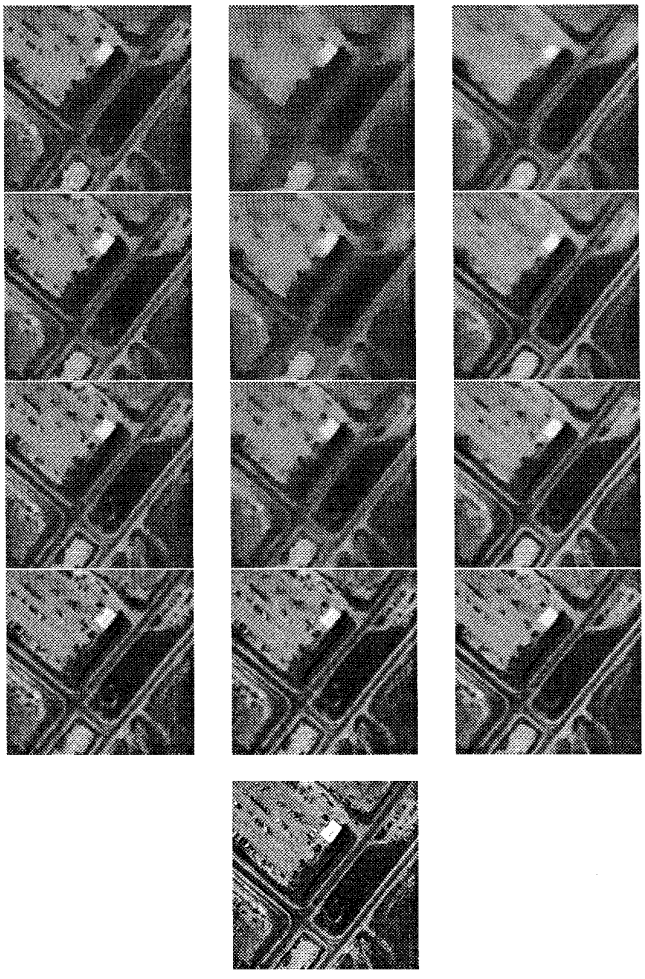

FIG. 14. A comparison of anisotropic diffusion [68] (left and middle columns) and curvature deformation (right column). Anisotropic diffusion is applied using the conductance function $g(\nabla\phi) = 1/(1 + (|\nabla\phi|/K)^2)$, where ϕ is the image intensity. Bottom: The original image is a portion of the aerial image in Fig. 13. Left column (bottom to top): Anisotropic diffusion, $K = 5$. When the conductance function drops sharply with increasing image intensity gradient, all sharp edges are preserved as the image is smoothed, including those of small structures such as the cars. Middle column (bottom to top): Anisotropic diffusion, $K = 10$. When the conductance function is less steep, small structures such as the cars are smoothed over. However, this is at the expense of also smoothing over the edges of larger structures such as the roads. Right column (bottom to top): Curvature deformation exhibits the property of smoothing over small structures such as the cars, because typically their contours have high curvature portions, while preserving slowly curving contours of larger structures such as the roads.

iso-intensity contours, exhibits the property of smoothing over small structures such as the cars, because typically their contours have high curvature portions, while preserving slowly curving edges of larger structures such as the roads (right column).

ACKNOWLEDGMENTS

This research was supported by NSF Grant IRI 9225139. The authors thank Steven W. Zucker for many discussions and Perry Stoll for some of the implementations. The medical images were kindly provided by Michael Stryker from UCSF. The aerial image is from the ARPA RADIUS program.

REFERENCES

1. L. Alvarez, F. Guichard, P. Lions, and J. Morel, Axiomatisation et nouveaux operateurs de la morphologie mathematique, *C. R. Acad. Sci. Paris* **315,** 1992, 265–268.
2. L. Alvarez, F. Guichard, P.-L. Lions, and J.-M. Morel, Axiomes et equations fondementales du traitement d'images (analyse multi-echelle at e.d.p), *C. R. Acad. Sci. Paris* **1,** 1992, 135–138.
3. L. Alvarez, F. Guichard, P.-L. Lions, and J.-M. Morel, Axioms and fundamental equations of image processing. *Arch. Rational Mech. Anal.* **123,** 1993, 199–257.
4. L. Alvarez and L. Mezzora, Signal and image restoration using shock filters and anisotropic diffusion, *SIAM J. Numer. Anal.* **31,** 1994.
5. L. Alvarez, P.-L. Lions, and J.-M. Morel, Image selective smoothing and edge detection by nonlinear diffusion: II, *SIAM J. Numer. Anal.* **29**(3), June 1992, 845–866.
6. L. Alvarez and J.-M. Morel, Formalization and computational aspects of image analysis, *Acta Numer.* 1994, 1–59.
7. A. Arehart, L. Vincent, and B. B. Kimia, Mathematical morphology: The Hamilton–Jacobi connection, in *Fourth International Conference on Computer Vision, Germany, Berlin, May 11–13, 1993,* Computer Society Press, Washington, DC, 1993.
8. H. Asada and M. Brady, The curvature primal sketch, *IEEE Trans. Pattern Anal. Machine Intell.* **8,** 1983, 2–14.
9. J. Babaud, A. P. Witkin, M. Baudin, and R. O. Duda, Uniqueness of the Gaussian kernel for scale-space filtering. *IEEE Trans. Pattern Anal. Machine Intell.* **8**(1), January 1986, 26–33.
10. G. Barles, Remarks on a flame propagation model, Technical Report 464, INRIA Rapports de Recherche, December 1985.
11. H. Blum, Biological shape and visual science, *J. Theor. Biol.* **38,** 1973, 205–287.
12. F. Catté, P.-L. Lions, J.-M. Morel, and T. Coll, Image selective smoothing and edge detection by nonlinear diffusion. *SIAM J. Numer. Anal.* **29**(1), February 1992, 182–193.
13. Y. Chen, Y. Giga, and S. Goto, Remarks on viscosity solutions for evolution equations, *Proc. Japan Acad.* **67**(Ser. A), 1991, 323–328.
14. Y. Chen, Y. Giga, and S. Goto, Uniqueness and existence of viscosity solutions of generalized mean curvature flow equations, *J. Diff. Geom.* **33**(3), 1991, 749–786.
15. M. Crandall, L. Evans, and P. Lions, Some properties of viscosity solutions of Hamilton–Jacobi equations, *Trans. Am. Math. Soc.* **282,** 1984, 487–502.
16. M. G. Crandall, H. Ishii, and P.-L. Lions, User's guide to viscosity solutions of second order partial differential equations, *Bull. Am. Math. Soc.* **27**(1), 1992, 1–67.
17. M. G. Crandall and P.-L. Lions, Viscosity solutions of Hamilton–Jacobi equations, *Trans. Am. Math. Soc.* **277,** 1983, 1–42.
18. H. Delingette, Intrinsic stabilizers of planar curves, in *Proceedings, Third European Conference on Computer Vision, Stockholm, 1994* (J. O. Eklundh, Ed.), pp. 427–436, Springer-Verlag, Berlin/New York, 1994.

19. M. P. do Carmo, *Differential Geometry of Curves and Surfaces,* Prentice Hall, NJ, 1976.
20. C. Epstein and M. Gage, The Curve Shortening Flow, in *Wave Motion: Theory, Modelling and Computation,* (A. Chorin and A. Majda Eds.), Springer-Verlag, New York, 1987.
21. L. C. Evans and J. Spruck. Motion of level sets by mean curvature I. *J. Diff. Geom.* **33**(3), May 1991, 635–681.
22. L. C. Evans and J. Spruck, Motion of level sets by mean curvature II, *Trans. Am. Math. Soc.* **330,** 1992, 321–332.
23. L. C. Evans and J. Spruck, Motion of level sets by mean curvature III, *J. Geom. Analysis* **2,** 1992, 121–150.
24. L. M. J. Florack, A. H. Salden, B. M. ter Haar Romeny, J. J. Koenderink, and M. A. Viergever, Nonlinear scale-space, In *Geometry-Driven Diffusion in Computer Vision,* pp. 339–370, Kluwer Academic, Dordrecht/Norwell, MA, 1994.
25. L. M. J. Florack, B. M. ter Haar Romeny, J. J. Koenderink, and M. A. Viergever, Linear scale-space, Technical Report 3DCV 93-02, 3D Computer Vision Research Group, Utrecht University, 1993.
26. M. Gage, An isoperimetric inequality with applications to curve shortening, *Duke Math. J.* **50,** 1983, 1225–1229.
27. M. Gage, Curve shortening makes convex curves circular, *Invent. Math.* **76,** 1984, 357–364.
28. M. Gage, On an area-preserving evolution equation for plane curves, *Contemp. Math.* **51,** 1986, 51–62.
29. M. Gage and R. S. Hamilton, the heat equation shrinking convex plane curves, *J. Diff. Geom.* **23,** 1986, 69–96.
30. Y. Giga and S. Goto, Motion of hypersurfaces and geometric equations, *J. Math. Soc. Jpn.* **44**(1), 1992, 99–111.
31. M. A. Grayson, The heat equation shrinks embedded plane curves to round points, *J. Diff. Geom.* **26,** 1987, 285–314.
32. A. Harten, High resolution schemes for hyperbolic conservation laws, *J. Comput. Phys.* **49,** 1983, 357–393.
33. E. Hopf, The partial differential equation $u_t + uu_x = \varepsilon u_x x$, *Commun. Pure Appl. Math.* **3,** 1950, 201–230.
34. B. Horn and E. Weldon, Filtering closed curves, *IEEE Trans. Pattern Anal. Machine Intell.* **8**(5), 1986.
35. R. Hummel, B. B. Kimia, and S. W. Zucker. Deblurring gaussian blur, *Comput. Vision Graphics Image Process.* **38,** 1987, 66–80.
36. H. Ishii, On uniqueness and existence of viscosity solutions of fully nonlinear second-order elliptic pde's, *Commun. Pure Appl. Math.* **42,** 1989, 15–45.
37. R. Jensen, The maximum principle for viscosity solutions of fully nonlinear second-order partial differential equations, *Arch. Rational Mech. Anal.* **101,** 1988, 1–27.
38. B. B. Kimia, Conservation laws and a theory of shape, Ph.D. dissertation, McGill Centre for Intelligent Machines, McGill University, Montreal, Canada, 1990.
39. B. B. Kimia, A. R. Tannenbaum, and S. W. Zucker, Toward a computational theory of shape: An overview, CIM-89-13, McGill Centre for Intelligent Machines, McGill University, Montreal, Canada, 1989.
40. B. B. Kimia, A. R. Tannenbaum, and S. W. Zucker, Reaction-diffusion equations and shape, in *Proceedings, British Conference on Computer Vision, Britain, 1990.*
41. B. B. Kimia, A. R. Tannenbaum, and S. W. Zucker, Toward a computational theory of shape: An overview, in *Proceedings, First European Conference on Computer Vision* (O. Faugeras, Ed.), pp. 402–407, Springer Verlag, Berlin, 1990.
42. B. B. Kimia, A. R. Tannenbaum, and S. W. Zucker, Entropy scale-space, *Visual Form: Analysis and Recognition* (C. Arcelli, Ed.) pp. 333–344, Plenum, New York, 1991.
43. B. B. Kimia, A. R. Tannenbaum, and S. W. Zucker, Exploring the shape manifold: The role of conservation laws, in *Proceedings, the Shape in Picture NATO Conference, September 1992.*
44. B. B. Kimia, A. R. Tannenbaum, and S. W. Zucker, On the evolution of curves via a function of curvature, I: The classical case. *JMAA* **163**(2), Jan. 1992.
45. B. B. Kimia, A. R. Tannenbaum, and S. W. Zucker, The shape triangle: Parts, protrusions, and bends, Technical Report TR-92-15, McGill University Research Center for Intelligent Machines, 1992.
46. B. B. Kimia, A. R. Tannenbaum, and S. W. Zucker, Non-linear shape approximation via the entropy scale space, in *Proceedings, SPIE's Geometric Methods in Computer Vision II, San Diego, CA, July 1993,* Vol. 2031, pp. 218–233.
47. B. B. Kimia, A. R. Tannenbaum, and S. W. Zucker, Shapes, shocks, and deformations, I: The components of shape and the reaction-diffusion space, *Int. J. Comput. Vision* **15**(3), 1995, 189–224.
48. J. J. Koenderink, The structure of images, *Biol. Cybernetics* **50,** 1984, 363–370.
49. J. J. Koenderink and A. J. van Doorn, Visual detection of spatial contrast: Influence of location in the visual field, target extent and illuminance level, *Biol. Cybernetics* **30,** 1978, 157–167.
50. J. J. Koenderink and A. J. van Doorn, Dynamic shape, *Biol. Cybernetics* **53,** 1986, 383–396.
51. P. D. Lax, *Hyperbolic Systems of Conservation Laws and the Mathematical Theory of Shock Waves,* SIAM Regional Conference series in Applied Mathematics, Philadelphia, 1973.
52. T. Lindeberg, Scale-space for discrete signals, *IEEE Trans. Pattern Anal. Machine Intell.* **12**(3), 1990, 234–254.
53. T. Lindeberg and J. Eklundh, Scale detection and region extraction from a scale-space primal sketch, in *Third International Conference on Computer Vision, Osaka, Japan, Dec. 4–7, 1990,* pp. 416–426, Computer Society Press, Washington, DC, 1990.
54. T. Lindeberg and B. M. ter Haar Romeny, Linear scale space I: Basic theory, in *Geometry-Driven Diffusion in Computer Vision,* (B. M. ter Haar Romeny, Ed.), pp. 1–38, Kluwer, Academic, Dordrecht/Norwell, MA, 1994.
55. T. Lindeberg and B. M. ter Haar Romeny, Linear scale space II: Early visual operations, in *Geometry-Driven Diffusion in Computer Vision* (B. M. ter Haar Romeny, Ed.), pp. 39–72, Kluwer, Academic, Dordrecht/Norwell, MA, 1994.
56. P. Lions, *Generalized Solutions of Hamilton Jacobi Equations,* Pitman, London, 1981.
57. D. G. Lowe, Organization of smooth image curves at multiple scales, in *Second International Conference on Computer Vision, Tampa, FL, December 5–8, 1988,* pp. 558–567, Computer Society Press, Washington, DC, 1988.
58. D. Marr and E. Hildreth, Theory of edge detection, Technical Report MIT AI Memo 518, MIT AI Lab, 1979.
59. Y. Meyer, *Wavelets and Operators,* Cambridge Univ. Press, Cambridge, UK, 1989.
60. F. Mokhtarian and A. Mackworth, Scale-based description of planar curves and two-dimensional shapes, *IEEE Trans. Pattern Anal. Machine Intell.* **8,** 1986, 34–43.
61. F. Mokhtarian and A. Mackworth, A theory of multiscale, curvature-based shape representation for planar curves, *IEEE Trans. Pattern Anal. Machine Intell.* **14**(8), August 1992, 789–805.
62. W. J. Niessen, B. M. ter Haar Romeny, L. M. J. Florack, A. H. Salden, and M. A. Viergever, Nonlinear diffusion of scalar images using well-posed differential operators, In *CVPR'94, IEEE Computer Society Conference on Computer Vision and Pattern Recognition, Seattle, Washington, June 20–23, 1994.*

63. N. Nordström, Biased anisotropic diffusion—A unified regularization and diffusion approach to edge detection, In *Proceedings of the First European Conference on Computer Vision* (O. Faugeras, Ed.), pp. 18–27, Springer Verlag, Berlin, 1990.
64. J. Oliensis, Local reproducible smoothing without shrinkage, *IEEE Trans. Pattern Anal. Machine Intell.* **15**(3), March 1993, 307–312.
65. S. Osher and S. Chakravarthy, High resolution schemes and the entropy condition, *SIAM J. Numer. Anal.* **21,** 1984, 955–984.
66. S. Osher and L. I. Rudin, Feature-oriented image enhancement using shock filters, *SIAM J. Numer. Anal.* **27**(4), Aug. 1990, 919–940.
67. S. Osher and J. Sethian, Fronts propagating with curvature dependent speed: Algorithms based on Hamilton–Jacobi formulations, *J. Comput. Phys.* **79,** 1988, 12–49.
68. P. Perona and J. Malik, Scale-space and edge detection using anisotropic diffusion, *IEEE Trans. Pattern Anal. Machine Intell.* **12**(7), July 1990, 629–639.
69. M. Proesmans, E. J. Pauwels, L. J. V. Gool, T. Moons, and A. Oosterlinck, Image enhancement using non-linear diffusion, Technical report, Katholieke Universiteit Leuven, Belgium, Dec. 1992.
70. M. H. Protter and H. F. Weinberger, *Maximum Principles in Differential Equations,* Springer-Verlag, New York, 1984.
71. A. Rosenfeld and M. Thurston, Edge and curve detection for visual scene analysis, *IEEE Trans. Comput.* **C-20,** 1971, 562–569.
72. G. Sapiro and A. Tannenbaum, Affine invariant scale-space, *Int. J. Comput. Vision* **10,** 1993, 25–44.
73. G. Shapiro and A. Tannenbaum, On invariant curve evolution and image analysis, *Indiana Univ. J. Math.,* to appear.
74. G. Sapiro and A. Tannenbaum, Area and length preserving geometric invariant scale-spaces, in *Proceedings, Third European Conference on Computer Vision* (J.-O. Eklundh, Ed.), pp. 449–458, Springer Verlag, Stockholm, 1994.
75. G. Sapiro and A. Tannenbaum, On affine plane curve evolution, *J. Functional Anal.* **119,** 1994, 79–120.
76. J. Sethian, An analysis of flame propagation, Ph.D. dissertation, University of California, Berkeley, Berkeley, CA, 1985.
77. J. Sethian, *Numerical Methods for Propagating Fronts,* pp. 155–164. Springer-Verlag, New York, 1985.
78. J. Sethian, A review of recent numerical algorithms for hypersurfaces moving with curvature dependent speed, *J. Diff. Goem.* (33), 1989, 131–161.
79. J. Sethian and S. Osher, *The Design of Algorithms for Hypersurfaces Moving with Curvature-Dependent Speed,* Springer Verlag, Berlin/ New York, 1988.
80. J. A. Sethian, Curvature and the evolution of fronts, *Commun. Math. Physics* **101,** 1985, 487–499.
81. J. Shah, Segmentation by nonlinear diffusion, in *CVPR'91, IEEE Computer Society Conference on Computer Vision and Pattern Recognition, Maui, HI, June 3–6, 1991,* pp. 202–207, Computer Society Press, Washington, DC, June 1991.
82. P. Stoll, C. Shu, and B. B. Kimia, Shock capturing numerical methods for partial differential equations arising in computer vision, Technical Report 132, Brown University, LEMS, May 1994.
83. D. Terzopoulos, Regularization of inverse visual problems involving discontinuities, *IEEE Trans. Pattern Anal. Machine Intell.* **8,** July 1986, 413–424.
84. R. T. Whitaker, Geometry-limited diffusion in the characterization of geometric patches in images, *Comput. Vision Graphics Image Process.* **57,** Jan. 1993, 111–120.
85. R. T. Whitaker and S. M. Pizer, A multi-scale approach to nonuniform diffusion, *Comput. Vision Graphics Image Process.* **57**(1), Jan. 1993, 99–110.
86. B. White, Some recent developments in differential geometry, *Math. Intelligenecer* **11**(4), 1989, 11–47.
87. D. Widder, *The Heat Equation,* Academic Press, San Diego, 1975.
88. A. P. Witkin, Scale-space filtering, in *Proceedings, 8th International Joint Conference on Artificial Intelligence, Karlsruhe, West Germany, August 1983,* pp. 1019–1022.
89. A. I. Yuille and T. A. Poggio, Scaling theorems for zero crossings, *IEEE Trans. Pattern Anal. Machine Intell.* **8**(1), Jan. 1986, 15–25.
90. S. W. Zucker and R. Hummel, Receptive fields and the representation of visual information. *Human Neurobiol.* **5,** 1986, 121–128.